

Less singular quasicrystals: life in low codimensions

A. Jagannathan

Laboratoire de Physique des Solides, Université Paris-Sud, 91405 Orsay, France
Department of Physics and Astronomy, University of Southern California, Los Angeles, USA

We consider a set of tilings proposed recently as d -dimensional generalisations of the Fibonacci chain, by Vidal and Mosseri. These tilings have a particularly simple theoretical description, making them appealing candidates for analytical solutions for electronic properties. Given their self-similar geometry, one could expect that the tight-binding spectra of these tilings might possess the characteristically singular features of well known quasiperiodic systems such as the Penrose or the octagonal tilings. We show here, by a numerical study of statistical properties of the tight-binding spectra that these tilings fall rather in an intermediate category between the crystal and the quasicrystal, *i.e.* in a class of almost integrable models. This is certainly a consequence of the low codimension of the new tilings.

INTRODUCTION

We report the results of a numerical study of the two-dimensional (2D) members of a new family of quasiperiodic tilings proposed recently by Vidal and Mosseri [1]. These new so-called generalized Rauzy tilings (GRT) (after the work of [2]), are generalizations of the Fibonacci chain and are simpler in structure than hitherto studied tilings in two and three dimensions. Tight-binding models on these systems may be amenable to analytical techniques whereas other 2D tilings thus far studied have been refractory to approaches including renormalization group, or recursive methods [3,4]. This property makes the new tilings attractive candidates to study in the world of quasiperiodic Hamiltonians. It is thus interesting to examine whether the tight-binding spectrum of these new tilings have similarly complex structures as for the “canonical” cases studied earlier, namely the Penrose or the Ammann-Beenker (octagonal) tilings. This turns out not to be the case: these tilings fall in a class intermediate between the periodic lattice, an integrable problem, and the octagonal tiling, which belongs in the non-integrable class.

This conclusion is based on calculations of statistical properties of the energy levels of periodic approximants of these new systems. Such analyses have been carried out for complex systems, including disordered media, systems with interactions or quantum billiards [5]. A relation is found to exist between the quantum statistics and the classical dynamics : depending on whether the dynamics is classically ergodic, or classically chaotic, one finds their quantum properties to be described by Poisson statistics or by Random Matrix Theory (RMT) [6]. Such statistical

analyses are useful for gaining insight into complex systems for which exact, or even approximate theoretical results are not available. This is the case for the octagonal tiling, a quasiperiodic tiling in two dimensions which has been tackled via numerical study of tight-binding models [7–9]. We show that the GRT in two dimensions has spectral properties that differ *essentially* from those of the octagonal tiling. The GRT appears analogous to the pseudointegrable billiards proposed in [10] which are neither completely integrable nor completely chaotic.

DESCRIPTION OF THE NEW TILINGS

The cut-and-project method provides a simple and easily implemented way to obtain pieces of quasiperiodic tilings. One can thus obtain arbitrarily large pieces of an infinite quasicrystal, or one can construct finite pieces that can be periodically continued – these are the periodic approximants of the quasicrystal. As described in [11], one first defines the real-space directions, which constitute a d -dimensional subspace of a larger D -dimensional hyperspace. The remaining $D-d$ directions constitute the “perpendicular” space. The quasicrystal is obtained by projecting all the points contained within a certain infinite strip in the hyperspace [12] onto the real space.

When the orientation of the real space is irrational, the tiling is aperiodic, while if rational orientations are chosen, the tiling repeats periodically in real space. This method has been used to obtain the Fibonacci chain ($D=2, d=1$), the octagonal tiling ($D=4, d=2$), the three-dimensional Penrose tiling ($D=6, d=3$) etc. The codimension, $D-d$, is in fact equal to d in the three cited cases.

The simplifying feature of the GRT [1] is that their codimension is equal to 1 for all real space dimension d . For a finite tiling, this allows one to index the points according to their perpendicular space coordinate. Furthermore, when the points of an approximant of these tilings – illustrated for two dimensions in Fig.1 – are so indexed, the connectivity matrix of the approximant (assuming toroidal boundary conditions) takes on a very simple band-diagonal (Toeplitz) structure [1]. In the two dimensional case that we consider here, the nonzero matrix elements are situated at distances of F_{n-3}, F_{n-2} and F_{n-1} from the diagonal. The generalized Fibonacci numbers $\{F_n\}$ are obtained from a three term recursion relation $F_n = F_{n-1} + F_{n-2} + F_{n-3}$, with the initial con-

ditions $F_{-1} = 0; F_0 = F_1 = 1$. The ratio F_n/F_{n-1} tends to the value $\alpha \approx 1.839\dots$, solution of the equation $x^3 = x^2 + x + 1$. These matrices correspond to approximants of increasing size as n is increased.

The model we consider is a pure hopping tight-binding Hamiltonian,

$$H = \sum_{\langle i,j \rangle} t c_i^\dagger c_j + h.c. \quad (1)$$

where i, j in the sum correspond to pairs of sites linked by a bond in Fig.1. The hopping amplitude has been assumed to be independent of the linked sites and is set to unity. We consider the case of periodic boundary conditions, and take $k = 0$ where k is the Bloch vector. The resulting eigenvalue problem reduces to that of diagonalizing the connectivity matrix defined above. This was done using a Lanczos routine. The spectrum is expected to be symmetric for the infinite tiling, since it is bipartite. In addition, there is a discrete symmetry under an inversion in the perpendicular subspace [13]. This results in two subspaces of positive and negative parity respectively, and our analyses are carried out for each sector separately.

RESULTS

The spectral density $\rho(E)$ is shown in Fig.2a, with that of the octagonal tiling shown in 2b for comparison (the localized states of the latter at $E = 0$ have not been included in the figure). The density of states curves shown were obtained for given sample sizes assuming periodic boundary conditions, and illustrate the characteristic rapidly fluctuating behavior typical of these aperiodic tilings (similar curves were found in [1] and [7]). It is evident that while the GRT has an underlying smoothly varying component of $\rho(E)$ which is everywhere non-zero (notice the y-axis offset) whereas the octagonal tiling does not. Calculations on approximants of the 2D Penrose tiling show strong fluctuations as well with a multitude of gaps and pseudogaps [14].

The envelope of $\rho(E)$ of the GRT is in fact reminiscent of the density of states of the square lattice. One notes in Fig.1 that there are many regions in which sites of coordination number 4 are grouped together in this tiling. In contrast to the octagonal tiling, which also has a mean coordination number $\bar{z} = 4$, the fluctuations of geometry are less strong in the GRT. This is a result of the reduced codimension, and we see that in consequence the density of states has a much less singular structure as compared to the octagonal case.

Turning to the statistics of nearest neighbor level spacings, we investigate the distribution of $E_{i+1} - E_i$ where the E_i are the ordered set of energy levels of the Hamiltonian (1). In order to eliminate the trivial dependence of this quantity on variations of $\rho(E)$, one first carries

out an ‘‘unfolding’’ of the spectrum [15] to get the corrected level spacings [16]. This yields the unfolded spacings s_i whose mean value is equal to 1. The resulting distribution of spacings $P(s)$ is plotted in Fig.3a for the three largest systems studied, which contain 35738(L), 19513(M) and 10609(S) sites. The dashed line represents the Poisson e^{-s} decay, while the continuous line is the semi-Poisson form $P_{SP}(s) = 4s \exp(-2s)$. The latter has been proposed for pseudointegrable billiards and can be shown to correspond to a certain short range plasma model (SRPM) by Bogomolny et al [10]. These authors speculate that this type of statistics is a consequence of fractal structure of the wave functions in those systems. In the Anderson model, the critical level statistics were first shown to have the semi-Poisson distribution by Braun et al [17]. In another example of this universality class Evangelou and Pichard had considered the distribution of bandwidths and obtained the semi-Poisson form in the critical Harper model [18].

In Fig.3a one sees that there is a size-dependence in the fall-off in $P(s)$ at small s . For the largest size, the points appear to deviate substantially from the semi-Poisson curve. It will be interesting to calculate the next system size to see if the deviations are systematically upwards, i.e. towards the Poisson limit. The $P(s)$ resembles that obtained in [17] for periodic boundary conditions at the critical point of the Anderson model. In contrast to the random case however, in our case there is a size-dependence. It is important to note that the *degree* of unfolding matters here: nonunfolded spacings follow a simple Poisson law while progressively stronger unfolding causes the distribution to go over to the semi-Poisson form. In Fig.3b we present a semilog plot of the statistics of the maximally unfolded level spacings (where we renormalized each spacing by the locally averaged value over the nearest neighbor energy levels). The agreement with the semi-Poisson form is seen to be good over a wide range of values. At large s $P(s)$ falls off faster than exponentially in s , while at small s , there is a size dependent increase of $P(s)$ above the semi-Poisson value. We believe that these effects may be explained by the unfolding procedure, although boundary condition effects cannot be ruled out and further studies are needed to settle this issue.

This distribution in Fig.3a is very different from the one obtained for the octagonal tiling. For that tiling, unfolded spacings follow the Wigner-Dyson distribution for random matrices of the gaussian orthogonal ensemble (GOE), $P_{GOE}(s) = \frac{\pi}{2} \exp(-\pi s^2/4)$. If one considers the distribution of the ‘‘bare’’ spacings (i.e. without correcting for the variation in density of states), they follow a broad (log-normal) distribution law : this can be shown via a recursive relation based on the inflation symmetry of the tilings [19]. A less singular case is that of a randomized version of the octagonal tiling [8]. The randomized tiling has a less fluctuating density of states and

the spacings distribution is simply GOE (unfolding does not produce any new effects). From these $P(s)$, as well as from the spectral rigidity function (to be discussed below) we conclude that the octagonal tilings belong in the class of non-integrable models exemplified by disordered metals. One has an unbounded diffusion of wave packets resulting in level repulsion at small s . The GRT is clearly not in the GOE regime for any scale of energies, rather it should be considered a nearly integrable system, as the shape of $P(s)$ indicates.

This becomes more evident upon looking at the spectral rigidity function $\Sigma^{(2)}(L) = \langle (N(L) - \bar{N})^2 \rangle$, where $N(L)$ is the number of levels lying within an energy interval of width L . The angular brackets mean averages over different starting positions of the interval within the spectrum. Fig.4a shows the plot of $\Sigma^{(2)}$ for the largest tiling size, for three different choices of unfolding [16]. The continuous line in Fig.4a indicates the SRPM result $\Sigma^{(2)}(L) = \frac{1}{2}(L + (1 - e^{-4L})/4)$. For very small L , the dependence appears well described by the semi-Poisson law. The three curves have the same low energy behavior, but the “most unfolded” case has its fluctuations damped out because of the unfolding, while the other cases show the transition from approximately linear to approximately quadratic dependence on L .

The SRPM behavior at small L may be related to a long time dynamics in this tiling which is intermediate between chaotic and integrable. This would correspond to the semi-Poisson form of $P(s)$. It is interesting to consider the rigidity evaluated for the energy levels without unfolding. In the case of random media, where diagrammatic perturbation theory can be exploited, and checked by more semiclassical methods [20], it was shown that in the diffusive regime, as a function of energy E , $\Sigma^{(2)}(E)$ has two different sorts of behavior: firstly, at very low energies, it has the logarithmic dependence expected for GOE matrices. This holds up to the scale of the Thouless energy E_c [21] which is size dependent, corresponding to the time taken to diffuse to the boundaries. For larger energies $\Sigma^{(2)} \sim E^{d\nu}$ where the exponent ν describes the spreading over time of an initially localized wave packet $\langle r^2 \rangle \sim t^{2\nu}$. This theoretical prediction was verified numerically in the Anderson model [22], where the exponent is one for ordinary diffusion, $\nu = 0.5$. For the randomized octagonal tiling, $\nu \approx 0.85$ [8] as deduced from $\Sigma^{(2)}$, in agreement with the results of a direct calculation of wavepacket diffusion on this tiling [23]. Fig.4b shows the log-log plot of $\Sigma^{(2)}$ as a function of energy for three sizes. There is a crossover from linear dependence to an almost quadratic dependence, $\Sigma^{(2)}(E) \propto E^{2\nu}$ ($\nu \approx 0.95$). The sub-quadratic regime very likely corresponds to the sub-ballistic regime of dynamics that was observed for wavepackets diffusing on a 2D GRT by Vidal and Mosseri [24].

DISCUSSION AND CONCLUSIONS

The two-dimensional GRT tiling, despite its quasiperiodic structure, is an almost integrable system, with a semi-Poisson form for the level spacings distribution and a corresponding small-energy spectral rigidity function. The $P(s)$ distribution is probably linked to the existence of fractal wavefunctions, as has already been observed in critical quantum systems. In the GRT studied here, it is noteworthy that although fluctuations of the density of states are present, they are strongly reduced with respect to those in “canonical” quasiperiodic tilings. This is a consequence of the reduced codimension of the tilings, which leads to its having weaker quasiperiodic modulations of geometry than the previously studied octagonal and Penrose tilings. Further study is needed to elucidate the nature of states and of the relation between dynamical evolution of wavepackets and the calculated statistical properties of the energy levels.

ACKNOWLEDGMENTS

I would like to acknowledge useful discussions with Frederic Piechon and Michel Duneau. I thank the computing center at IDRIS, Orsay for the computing facilities and support needed for this study.

-
- [1] J. Vidal and R. Mosseri, J.Phys.Math. Gen. **34** 3927 (2001); J. Vidal and R. Mosseri, Proceedings of ICQ7, Mat.Sci. and Engg. **294-296** 572 (2000)
 - [2] G. Rauzy, Bull. Soc. Math. France **110**, 147 (1982)
 - [3] J. X. Zhong and R. Mosseri, J.Phys.(France) **4**, 1513 (1994)
 - [4] A. Jagannathan, J.Phys.(France) **I4**, 133 (1994)
 - [5] Mesoscopic Quantum Physics, Proceedings of Les Houches Summer School eds. E. Akkermans et al (Elsevier, 1996); Chaos and Quantum Physics, Proceedings of Les Houches Summer School, eds. M.J. Giannoni, A. Voros and J. Zinn-Justin, (Elsevier, New York 1991)
 - [6] M. L. Mehta, Random Matrices (Academic New York, 1991)
 - [7] V. G. Benza and C. Sire, Phys. Rev. B**44**, 10343 (1991)
 - [8] F. Piechon and A. Jagannathan, Phys.Rev.B **51** 179 (1995);
 - [9] J. X. Zhong et al, Phys. Rev. Lett.**80** 3996 (1998)
 - [10] E. Bogomolny, U. Gerland and C. Schmit, Phys. Rev. E **59**, R13 15 (1999)
 - [11] M. Duneau and A. Katz, Phys. Rev. Lett. **54**, 2688 (1985); P. A. Kalugin, A. Y. Kitaev, and L. S. Levitov, J. Phys. (Paris) Lett. **46**, L601 (1985); M.Duneau, R.Mosseri, and C.Oguey, J. Phys. A **22**, 4549 (1989)

- [12] The strip is defined by the set of points whose perpendicular space coordinates lie within a finite “acceptance domain”.
- [13] The Hamiltonian is invariant under a reindexation of points given by inversion of the perpendicular space coordinate with respect to the midpoint of the strip. This symmetry is not exactly obeyed in the approximants, however the symmetry breaking gets weaker as system size is increased.
- [14] E.S. Zijlstra and T. Janssen, Phys. Rev. B **61** 3377 (2000)
- [15] O. Bohigas and M.J. Giannoni, in Mathematical and Computational Methods in Nuclear Physics eds. J.S.Dehesa, J.M.G. Gomez and A. Polls (Springer Lecture Notes vol.209, Berlin 1984)
- [16] The smoothed integrated density of states is calculated using a spline fit on a subset of the data points. The more points used in the smoothing, the greater the “unfolding”.
- [17] D. Braun, G. Montambaux and M. Pascaud, Phys. Rev. Lett. **81** 1062 (1998)
- [18] S. N. Evangelou and J.L. Pichard, Phys. Rev. Lett. **84**, 1643 (2000)
- [19] A. Jagannathan, Phys. Rev. B **61** R834 (2000)
- [20] B. L. Altshuler and B. I. Shklovskii, JETP **64**, 127 (1986); N. Argaman, Y. Imry and U. Smilansky, Phys. Rev. B **47**, 4440 (1993)
- [21] D. J. Thouless, Phys. Rev. Lett. **39**,1167 (1977)
- [22] D. Braun and G. Montambaux, Phys. Rev.B **52** 13903 (1995)
- [23] B. Passaro, C. Sire, and V. G. Benza, Phys. Rev. B **46**, 13751 (1992).
- [24] J. Vidal, thesis University of Paris 6, 1999

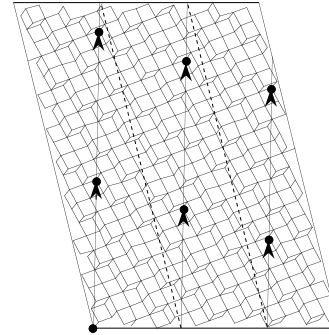


FIG. 1. An approximant of the 2D rauzy tiling showing the numbering scheme: the arrows show the displacement vector from site 0(origin) to site 1, etc. Note the periodic boundary conditions.

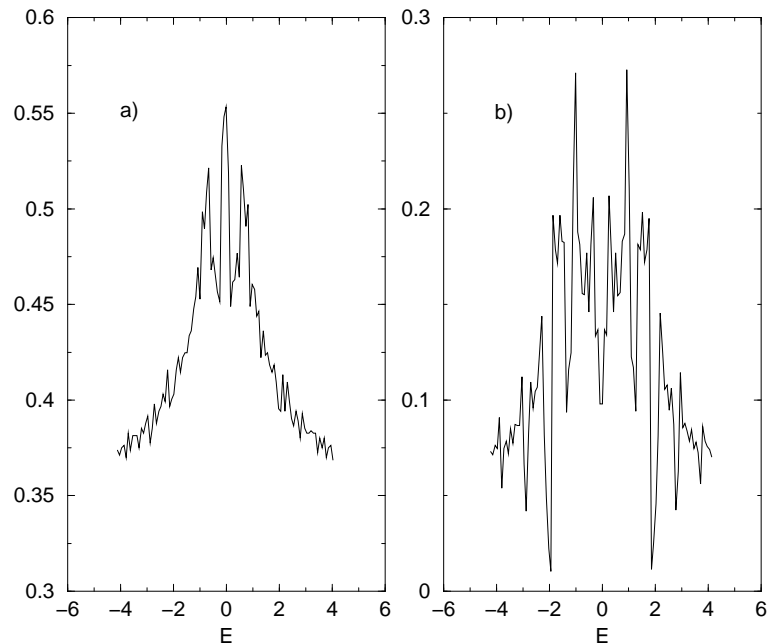


FIG. 2. (a) Density of states of the 2D Rauzy tiling and (b) of the octagonal tiling

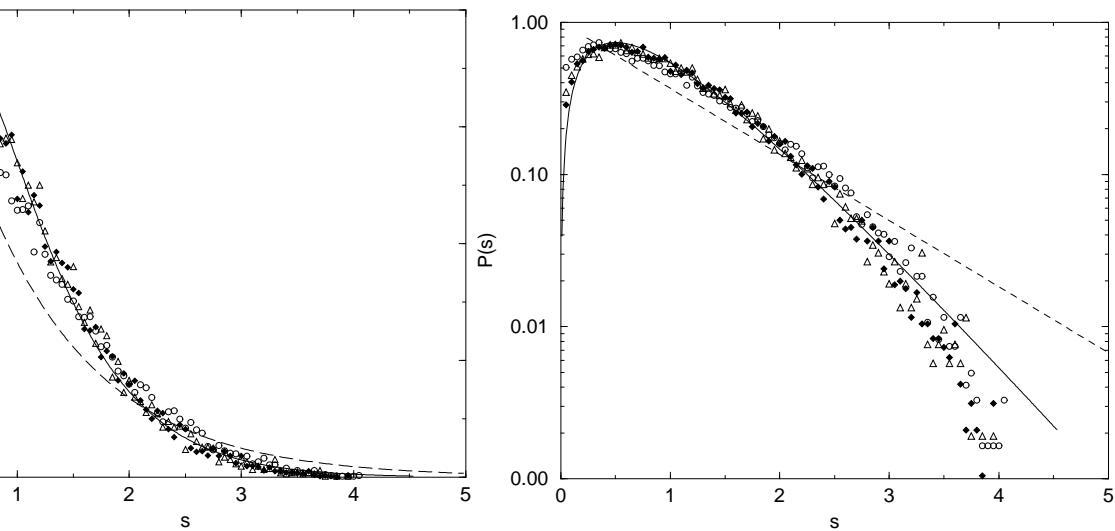


FIG. 3. (a) $P(s)$ of three approximants: L(circles), M(diamonds) and S(triangles) along with the semi-Poisson (continuous line) and the Poisson (dashed line) laws. (b) Semilog plots of $P(S)$ with the Poisson and the semi-Poisson laws (dashed and continuous lines respectively).

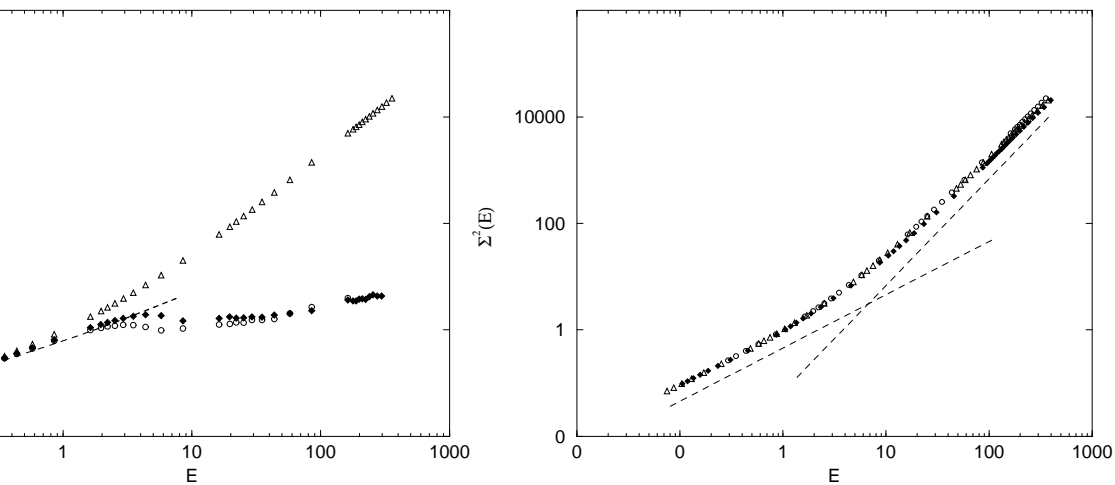


FIG. 4. (a) The rigidity $\Sigma^2(E)$ for different levels of unfolding, (see text) from most unfolded (circles) to not unfolded (triangles). (b) $\Sigma^2(E)$ without unfolding for three sizes L, M and S. The dashed lines show E and E^2 power laws.